Modeling the Localized-to-Itinerant Electronic Transition in the Heavy Fermion System CeIrIn$_5$

J. H. Shim, K. Haule, G. Kotliar

Center for Materials Theory, Department of Physics and Astronomy, Rutgers University, Piscataway, NJ 08854, USA.

We address the fundamental question of crossover from localized to itinerant state of a paradigmatic heavy fermion material CeIrIn$_5$. The temperature evolution of the one electron spectra and the optical conductivity is predicted from first principles calculation. The buildup of coherence in the form of a dispersive many body feature is followed in detail and its effects on the conduction electrons of the material is revealed. We find multiple hybridization gaps and link them to the crystal structure of the material. Our theoretical approach explains the multiple peak structures observed in optical experiments and the sensitivity of CeIrIn$_5$ to substitutions of the transition metal element and may provide a microscopic basis for the more phenomenological descriptions currently used to interpret experiments in heavy fermion systems.

Heavy fermion materials have unusual properties arising from the presence of a partially filled shell of f-orbitals and a very broad band of conduction electrons. At high temperatures, the f-electrons behave as atomic local moments. As the temperature is reduced, the moments combine with the conduction electrons to form a fluid of very heavy quasiparticles, with masses which are two to three orders of magnitude larger than the mass of the electron (*1*, *2*).

These heavy quasiparticles can undergo superconducting or magnetic transitions at much lower temperatures. Understanding how the itinerant low energy excitations emerge from the localized moments of the f shell is one of the central challenges of the condensed matter physics. It requires the understanding of how the dual, atomic particle-like and itinerant wave-like, character of the electron manifests itself in the different physical properties of a material.

CeIrIn$_5$ (*3*) has a layered tetragonal crystal structure (*4*, *5*) (Fig. 1A) in which the layers of CeIn$_3$ (shown as red and gray spheres) are stacked between layers of IrIn$_2$ (yellow and grey spheres). Each Ce atom is surrounded by four In atoms in the same plane and eight In atoms out of plane.

To describe the electronic structure of these class of materials, one needs to go beyond the traditional concepts of bands and atomic states, and focus on the concept of a spectral function $A(\mathbf{k},\omega)_{LL}$, which describes the quantum

mechanical probability of removing or adding an electron with angular momentum and atomic character $L = (l,m,a)$, momentum $\mathbf{k}$ and energy ω. It is measured directly in angle resolved photoemission and inverse photoemission experiments.

To evaluate the spectral function we use Dynamical Mean Field Theory (DMFT) (*6*) in combination with the Local Density Approximation (LDA+DMFT) (*7*) which can treat the realistic band structure, the atomic multiplet splitting and Kondo screening on the same footing. The spectral function is computed from corresponding one-electron Green's function $A(\mathbf{k},\omega) = (G^\dagger(\mathbf{k},\omega)-G(\mathbf{k},\omega))/(2\pi i)$ where the latter takes the form

$$G(\mathbf{k},\omega) = \frac{1}{(\omega+\mu)O_{\mathbf{k}} - H_{\mathbf{k}} - \Sigma(\omega)}. \quad (1)$$

Here $H_{\mathbf{k}}$ and $O_{\mathbf{k}}$ are the Hamiltonian and overlap matrix obtained by the LDA method (*8*) and Σ is the DMFT self-energy, which requires a solution of the quantum impurity problem embedded in a self consistent medium. We used a vertex corrected one-crossing approximation (*7*) and the results were further crosschecked against a continuous time quantum Monte Carlo method (*9*, *10*). The Slater integrals, F2,F4,F6, were computed by the atomic physics program of (*11*) and F0 was estimated by the constrained LDA to be 5 eV (*12*). The localized Ce-4f-orbital was constructed from the non-orthogonal Linear-Muffin-Tin-orbitals in particular way to maximize its f character, as explained elsewhere (*13*).

The spectral function of f electron materials has been known to exhibit remarkable many body effects. To set the stage for their theoretical description, Fig. 1B displays the Ce-4f local spectral function, i.e., $A(\omega) = \sum_{\mathbf{k}}A(\mathbf{k},\omega)$, which is measured in angle integrated photoemission experiments. At room temperature, there is very little spectral weight at the Fermi level as the f electrons are tightly bound and localized on the Ce atom, giving rise to a broad spectrum concentrated mainly in the lower and upper Hubbard bands at –2.5 eV and +3 eV, respectively.

As the temperature is decreased, a narrow peak appears near the Fermi level (see Fig. 1B). The states forming this peak have a small but finite dispersion, and therefore the area of the peak can be interpreted as the degree of f electron

delocalization. This quantity as well as the scattering rate of the Ce-4f states (Im$\Sigma(\omega = 0)$) exhibit a clear crossover at a temperature scale T^* of the order of 50 K (Fig. 1C).

Our results are consistent with the angle integrated photoemission measurements (14) in which the onset of states with f character at the Fermi level were observed. But the experimental resolution has to be improved by one order of magnitude to resolve the narrow peak predicted by the theory.

We now turn to the total (traced over all orbitals) momentum resolved spectral function Tr[$A(\mathbf{k},\omega)$] plotted along symmetry directions in the Brillouin zone. In a band theory description, it would be sharply peaked on a series of bands $\varepsilon_n(\mathbf{k})$ and the weight of those peaks would be unity. It is worthwhile comparing the high intensity features of the LDA+DMFT spectra (color coded) with the LDA bands ($\varepsilon_n(\mathbf{k})$ - drawn in blue) (Fig. 2A). In the region below –1 eV, there is a good correspondence between them. Notice however the systematic down shift (indicated by a green arrow) of the LDA+DMFT features relative to the LDA bands (which have mainly In-5p and Ir-5d character). Surprisingly, a similar trend is seen in the angle resolved photoemission experiments (ARPES) of (15) which we redraw in Fig. 2B. The position of these bands is weakly temperature dependent and, if warmed to room temperature, an almost rigid upward shift of 5 meV was identified in our theoretical treatment. Experimentally, it was not possible to resolve the momentum in z direction therefore the same experimental data (which can be thought as the average of the two paths from Γ-X and Z-R) is repeated in the two directions.

Near the Fermi level (between –0.5 eV and +1 eV), there are significant discrepancies between the LDA bands (which in this region have significant f character) and the LDA+DMFT features. The correlations treated by LDA+DMFT substantially modify the spectral function features with f content, transferring spectral weight into the upper Hubbard band located around +3 eV (white region in Fig. 2A).

Hubbard bands are excitations localized in real space, without a well defined momentum, and therefore they show up as a blurred region of spectral weight in momentum plot of Fig. 2A. There is also a lower Hubbard band around –2.5 eV which is hardly detectable in this figure. The reason is that it carries a very small spectral weight which is redistributed over a broad frequency region as shown in Fig. 1B. It is also useful to compare the LDA+DMFT Hubbard bands with those obtained with more familiar LDA+U method. The latter method inserts a sharp non-dispersive band around –2.5 eV and significantly twists the rests of the conduction bands. For the purpose of describing the set of bands below –1 eV, the LDA+DMFT method, is therefore closer to the LDA type of calculation with f bands removed from the valence band.

To obtain further insights into the nature of the low energy spectra, we show in Fig. 2, C and D, the momentum resolved f electron spectral function of Fig. 1B. The two plots correspond to the low (10 K) and high (300 K) temperature spectra, respectively. At room temperature a set of broad and dispersive bands are seen, and should be interpreted as the spd bands leaving an imprint in the f electron spectral function due to hybridization. At low temperature, a narrow stripe of spectral weight appears at zero frequency, which cuts the conduction bands and splits them into two separate pieces, divided by a new hybridization gap.

The two straight non-dispersive bands at –0.3 eV and +0.3 eV can also be identified in Fig. 2C and are due to the spin-orbit coupling (16). The same splitting of the coherence peak can be identified in the local spectra plotted in Fig. 1B and was recently observed in ARPES study (14).

A detailed analysis of the zero energy stripe of spectra in Fig. 2C reveals that the low energy features correspond to the three very narrow bands (the dispersion is of the order of 3 meV) crossing the Fermi level. This is the origin of the large effective mass and large specific heat of the material at low temperatures. The low energy band structure and its temperature dependence are theoretical predictions which can be verified experimentally in future ARPES studies.

Optical conductivity is a very sensitive probe of the electronic structure and has been applied to numerous heavy fermion materials (17). It is a technique which is largely complementary to the photoemission, on two counts. It probes the bulk and not the surface, and it is most sensitive to the itinerant spd electrons, rather than the f electrons.

A prototypical heavy fermion at high temperatures has an optical conductivity, characterized by a very broad Drude peak. At low temperatures, optical data is usually modeled in terms of transitions between a two renormalized bands, separated by a hybridization gap. These two bands give rise to a very narrow Drude peak of small weight, and an optical absorption feature above the hybridization gap, termed mid-infrared peak. This picture qualitatively describes the experimental data of CeIrIn$_5$ (18, 19), which we reproduce in Fig. 3B. However, this simplified two band model fails to account for some aspects of the data. For example, at 10 K there is a clear structure in the mid-infrared peak. In addition to the broad shoulder around 0.07 eV, a second peak around 0.03 eV can be identified, which was previously interpreted as the absorption on the bosonic mode that might bind electrons in the unconventional superconducting state (18, 20).

Also the hybridization gap in simplified theories gives rise to a sharp drop of conductivity below the energy of the gap, while broader features are seen experimentally.

Optical conductivity within LDA+DMFT was recently implemented (21) and we show results in Fig. 3A. They bear

a strong resemblance to the experimental data Fig. 3B. For example a broad Drude peak at high temperature and a very clear splitting of the mid-infrared peak at low temperature.

To understand the physical origin of these multiple peaks we plot in Fig. 3, C and D, the momentum resolved conduction electron (non-Ce-4f) spectral function along a representative high-symmetry line at 10 K and 300 K, respectively. Notice the dramatic difference between the two temperatures. At high temperature, we see two bands in this momentum direction, one very broad and one narrower. The dispersion of the left band in Fig. 3D is due to electron electron scattering, which broadens the band for approximately 100 meV. The character of both bands is primarily of In-5p, with an important difference. The left band comes mostly from the In atoms in the IrIn$_2$ layer, while the right band is mostly due to In in the CeIn$_3$ layer. The latter In atoms will be called in plane (each Ce has 4 neighbors of this type) and the former out of plane (there are 8 nearest neighbors to Ce atom). As the temperature is lowered, the two In bands hybridize in very different way with the Ce 4f moment. It is very surprising that the in-plane In atoms hybridize less with Ce moment leading to a small hybridization gap of the magnitude 30 meV (blue arrow in Fig. 3A). The out of plane In are more coupled to Ce moment, which leads to larger hybridization gap of the order of 70 meV (green arrow in Fig. 1A). The existence of multiple hybridization gaps results in the splitting of the mid-infrared peak in optical conductivity shown in Fig. 3A.

The remarkable fact that the Ce moment is more coupled to out of plane In than in-plane In provides a natural explanation for why these materials are sensitive to substitution of transition metal ion Ir with Co or Rh. Namely, the out of plane In are not only strongly coupled to Ce but also to the transition metal ion in their immediate neighborhood, while the in-plane In are insensitive to the substitution.

Some of the results of the microscopic theory such as the momentum dependent hybridization (*19*) and the slow buildup of coherence (*22*) were forshadowed by earlier phenomenological approaches. The first principles DMFT treatment places these ideas within a microscopic framework.

In investigating the formation of the heavy fermion state with temperature in CeIrIn$_5$, we have shown that incorporating local correlations on the f site only, allows for a coherent description of the evolution of the one electron spectra and the optical conductivity with temperature. The approach, provides a natural explanation for many surprising features observed in this material, and makes a number of quantitative predictions for the evolution of the spectra as a function of temperature which can be tested by ARPES measurements currently under way. While the single site DMFT description is sufficient in a broad region of

temperatures and parameters, cluster extensions of DMFT will be necessary to address the quantum criticality that takes place as Ir is replaced by Rh and Co, and the possible instabilities towards unconventional superconductivity. While model cluster DMFT studies seem very promising, the implementation of these methods in conjunction with realistic electronic structure remains a challenge for the future. Furthermore, to treat other compounds of the same class (Ir substituted by Co or Rh), the correlations on the 3d or 4d transition metal will require GW to treat the electronic structure.

References and Notes

1. G. R. Stwart, *Rev. Mod. Phys.* **56**, 755 (1984).
2. J. W. Allen, *J. Phys. Soc. Japan*, **74**, 34 (2005).
3. C. Petrovic *et al.*, *Europhys. Lett.* **53**, (2001).
4. Y. N. Grin, Y. P. Yarmolyuk, E. I. Giadyshevskii, *Sov. Phys. Crystallogr.* **24**, 137 (1979).
5. E. G. Moshopoulou, Z. Fisk, J. L. Sarrao, J. D. Thompson, *J. Solid State Chem.* **158**, 25 (2001).
6. G. Kotliar, D. Vollhardt, *Physics Today* **57**, 53 (2004).
7. G. Kotliar *et al. Rev. Mod. Phys.* **78**, 865 (2006).
8. S. Y. Savrasov, *Phys. Rev. B* **54**, 16470 (1996).
9. P. Werner, A. Comanac, L. de' Medici, M. Troyer, A. J. Millis, *Phys. Rev. Lett.* **97**, 076405 (2006).
10. K. Haule, *Phys. Rev. B* **75**, 155113 (2007).
11. R. D. Cowan, *The Theory of Atomic Structure and Spectra* (Univ. California Press, Berkeley, 1981).
12. A. K. McMahan, C. Huscroft, R. T. Scalettar, E. L. Pollock, *J. Comput,-Aided Mater. Des.* **5**, 131 (1998).
13. A. Toropova, C. A. Marianetti, K. Haule, G. Kotliar, in press; preprint available at http://arxiv.org/abs/0708.1181.
14. S. I. Fujimori *et al.*, *Phys. Rev. B* **73**, 224517 (2006).
15. S. I. Fujimori *et al.*, *Phys. Rev. B* **67**, 144507 (2003).
16. A. Sekiyama *et al.*, *Nature* **403**, 396 (2000).
17. L. Degiorgi, *Rev. Mod. Phys.* **71**, 687 (1999).
18. F. P. Mena, D. van der Marel, J. L. Sarrao, *Phys. Rev. B* **72**, 045119 (2005).
19. K. S. Burch *et al.*, *Phys. Rev. B* **75**, 054523 (2007).
20. E. J. Singley, D. N. Basov, E. D. Bauer, M. B. Maple, *Phys. Rev. B* **65**, 161101(R) (2002).
21. K. Haule, V. Oudovenko, S. Y. Savrasov, G. Kotliar, *Phys. Rev. Lett.* **94**, 036401 (2005).
22. S. Nakatsuji, D. Pines, Z. Fisk, Two Fluid Description of the Kondo Lattice. *Phys. Rev. Lett.* **92**, 016401 (2004).
23. We are grateful to Shin-ichi Fujimori and Atsushi Fujimori for their published data of ARPES on CeIrIn$_5$, to F. P. Mena, D. van der Marel, J. L. Sarrao for their published data of optics on CeIrIn$_5$ and to Jim Allen for unpublished data on other heavy fermion compounds. Work supported by the NSF Division of Material Research (grant 0528969).

Fig. 1. (**A**) Crystal structure of CeIrIn$_5$. Red, gold, and gray spheres correspond Ce, Ir, and In atoms, respectively. (**B**) Ce 4f local density of state calculated by LDA+DMFT at 10 K and 300 K. (**C**) The quasiparticle peak hight versus temperature (blue), imaginary part of Ce 4$f_{5/2}$ self-energy $\Sigma_f(\omega = 0)$(red) and its temperature derivative (green). The buildup of coherence is very slow and gradual. Around $T^* \sim 50$ K the coherence first sets in and manifested itself in fast increase of the quasiparticle peak (blue line) and crossover in the scattering rate (the derivative of scattering rate - green line - is peaked at T^*). The quasiparticle peak weight saturates at much lower temperature < 5 K and drops to zero at very high temperature, displaying a very long logarithmic tail.
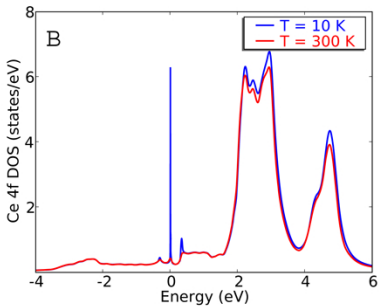
Fig. 2. (**A**) Momentum resolved total spectral functions calculated by LDA+DMFT method at 10 K is shown by color scheme. The LDA bands are drawn by blue lines. (**B**) Color plot shows experimental ARPES data reproduced from (*15*). Blue lines follow the LDA bands. (**C**) Momentum resolved Ce-4f spectral function at 10 K. (**D**) same as (C) but at 300 K.

Fig. 3. The optical conductivity at several temperatures (**A**) obtained by LDA+DMFT and (**B**) measured experimentally and reproduced from (*18*). The momentum resolved non-f spectral function ($A_{\text{total}} - A_{\text{Ce-4}f}$) at (**C**) 10 K and (**D**) and 300 K.